Available online at www.sciencedirect.com
SCIENCE DIRECT®
Journal of Nuclear Materials 324 (2004) 77–89
journal of nuclear materials
www.elsevier.com/locate/jnucmat

The change in tensile properties of wrought LCAC molybdenum irradiated with neutrons

B.V. Cockeram [a,*], J.L. Hollenbeck [a], L.L. Snead [b]

[a] Bettis Atomic Power Laboratory, Bechtel-Bettis, Inc., P.O. Box 79, West Mifflin, PA 15122-0079, USA
[b] Oak Ridge National Laboratory, P.O. Box 2008, Oak Ridge, TN 37831-6138, USA

Received 17 March 2003; accepted 20 May 2003

Abstract

Molybdenum alloys are known to be most susceptible to neutron radiation damage at radiation temperatures <800 °C, a condition which has limited their broader use in nuclear applications. Manipulation of alloy microstructure through the optimization of carbon and oxygen contents, and mechanical working were investigated as means to mitigate the undesirable effects of irradiation. Low carbon arc cast (LCAC) molybdenum sheet specimens were irradiated in the high flux isotope reactor (HFIR) at temperatures ranging from 270 to 1100 °C and at neutron fluences between 10.5 and 64.4×10^{24} n/m^2 ($E > 0.1$ MeV). Irradiation of LCAC molybdenum at nominal temperatures of 935–1100 °C produced only moderate changes in tensile strength, tensile elongation, and no change in the ductile to brittle transition temperature (DBTT) as inferred from tensile fracture surfaces. Irradiation of LCAC molybdenum at either 270 or 605 °C resulted in a significant increase in yield strength, a decrease in tensile elongation, and an increase in DBTT. This behavior is characteristic of that reported for pure molybdenum following irradiation at temperatures <800 °C. The use of arc-cast processing, a low oxygen content, and high carbon to oxygen ratio to produce the LCAC molybdenum used in this work results in strong grain boundaries that are not the preferred fracture path.

1. Introduction

The high melting point, creep-resistance and strength at high temperatures, and measurable tensile ductility of molybdenum at room-temperature have attracted interest for a number of applications [1–8]. Low carbon arc cast (LCAC) molybdenum is unalloyed molybdenum with low levels of oxygen and nitrogen impurity, and controlled amounts of carbon [9]. High ductility is observed for wrought arc-cast LCAC molybdenum that has a fine grain size when the carbon content is less than 100 ppm, the oxygen content is low, and a high ratio of carbon to oxygen is present [10–13]. Carbon serves to decrease the overall oxygen content and tie-up oxygen on the grain boundaries to prevent embrittlement, and form carbides that strengthen the grain boundaries. Although wrought molybdenum that has a fine grain size can possess relatively high amounts of tensile ductility and damage tolerance at room-temperature, neutron irradiation at temperatures <800 °C can result in a significant increase in the strength and decrease in tensile ductility [1–8]. This radiation embrittlement is characterized by an increase in the DBTT from below room-temperature in the unirradiated condition to values between 600 and 700 °C. The self-diffusion rate of point defects in molybdenum is sufficiently low at temperatures <800 °C that a high density of finely spaced point defect clusters and dislocation loops are produced by neutron irradiation of molybdenum that limit the homogeneous movement of dislocations and result in brittle fracture at low strains [1–3]. Since the mobility of point defects is larger at higher temperatures and diffusion to sinks can occur at a higher rate, a low net

* Corresponding author. Tel.: +1-412 476 5647; fax: +1-412 476 5151.
E-mail address: cockeram@bettis.gov (B.V. Cockeram).

0022-3115/$ - see front matter © 2003 Elsevier B.V. All rights reserved.
doi:10.1016/j.jnucmat.2003.05.001

accumulation rate of point defects is observed for the irradiation of molybdenum at temperatures >800 °C, which generally results in little change in the DBTT for irradiation at temperatures >800 °C.

The purpose of this work is to determine the influence of neutron radiation on the tensile properties of wrought LCAC molybdenum sheet that has a fine grain size. The change in mechanical properties with irradiation for different metallurgical conditions, including recrystallized and stress-relieved, and longitudinal and transverse orientation is also investigated.

2. Materials and experimental procedure

The reported compositions for LCAC molybdenum sheet that were fabricated by H.C. Starck, Inc. are reported in Table 1. Independent glow discharge mass spectrometry (GDMS) results obtained at Shiva Technology are generally within a factor of two of the chemical certification with the exception of oxygen. The higher oxygen content of the LCAC molybdenum sheet in the GDMS analysis may have resulted from the methods used to prepare the specimens for analysis. The most abundant tramp metallic elements are tungsten, iron, chromium, titanium, and nickel, with the highest levels observed for tungsten. LCAC molybdenum were produced using the processing methods that have been described [14,15]. After rolling the starting ingots into plate and then into sheet, the LCAC molybdenum sheet were given a final stress-relief anneal at 900 °C for 1 h in vacuum. Some of the LCAC specimens were recrystallized by a heat treatment of 1150 °C for 1 h. Four metallurgical conditions were evaluated: (1) longitudinal stress-relieved (LSR), (2) transverse stress-relieved (TSR), (3) longitudinal recrystallized (LR), and (4) transverse recrystallized (TR). Tensile specimens with a nominal thickness ranging from 0.76 to 0.40 mm (Fig. 1) were machined in the longitudinal or transverse orientation, laser scribed for identification, pickled, and electropolished [14]. The variation in thickness was on the order of 0.0025 mm for each individual tensile specimen. A final stress-relief anneal of 900 °C for 1 h for LCAC in vacuum was then performed.

Specimens were loaded into a rectangular axial opening machined into a 5.08 cm diameter × 5.6 cm long cylindrical specimen holder that was made of aluminum for the 270 °C irradiation or vanadium for the 605–1100 °C irradiation temperature. A filler piece of vanadium is placed in the gauge region of the tensile specimens to minimize the overall temperature gradient in the gauge region of the tensile specimens, which was determined from thermal calculations to be on the order of 10 °C at an irradiation temperature of 270 °C and on the order of 25 °C at an irradiation temperature of 1100 °C. The specimens, filler, specimen holder were centered within

Table 1
Chemical analysis of the LCAC molybdenum sheet used in this work (in weight percent ppm)

Material/lot#	C	O	N	Ti	Zr	Fe	Ni	Si	La	Al	Ca	Cr	Cu	Other
LCAC sheet, ingot 40386A2, heat# C18605, 0.51 mm sheet	90	3	4	NA	NA	10	<10	<10	NA	NA	NA	NA	NA	NA
LCAC specification[a]	⩽100	⩽15	⩽20	NA	NA	⩽100	⩽20	⩽100	NA	NA	NA	NA	NA	NA
GDMS data														
LCAC sheet	~100	~45	~2	8	0.95	20	2.2	1	<0.005	1.7	0.1	3.9	0.3	150 W

Note: NA = not available. All material was obtained from H.C. Stark, which was formally known as CSM Industries, Inc., Cleveland, OH. Trace GDMS composition for elements not listed was <1 ppm.

[a] ASTM B387-365 for arc-cast LCAC [9].

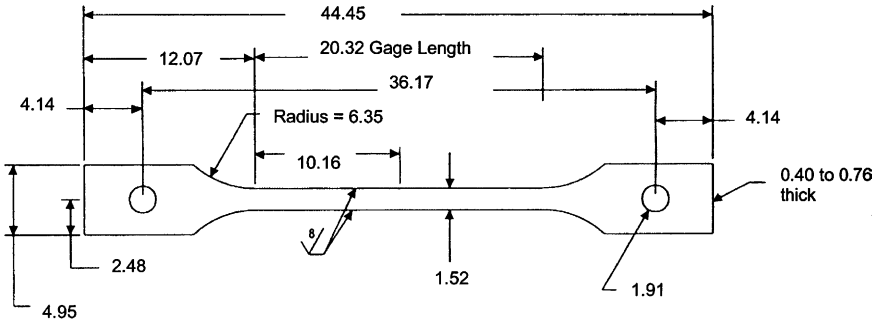

Fig. 1. Schematic of the SS-1 tensile specimen with nominal dimensions in mm.

an aluminum capsule using a thimble, and then welded in an inert helium atmosphere to form a hermetic seal. The majority of the heat produced in the specimen/holder is transferred to the capsule by conduction across the helium gas-gap, with only a small amount of heat lost from the centering thimbles to the capsule body. Heat generation rates, fabrication dimensions, temperature of the capsule, and the thermal expansion properties of the materials are used to develop a thermal model that was used to determine the temperature of the tensile specimen during irradiation, which is primarily based on the gas gaps within the capsule. Each capsule contained 10 tensile specimens.

The capsules were irradiated in the peripheral target tube position (PTP) of the high flux isotope reactor (HFIR) under the conditions given in Table 2 in one to three cycles between 15 June 2000 and 1 October 2000 at 85 MW of power: (1) cycle 380 for 2230 MW days (26.2 days of operation), (2) cycle 381 for 2123 MW days (25.0 days of operation), and (3) cycle 382 for 1755 MW days (20.6 days of operation). Most of the low fluence irradiations were completed in cycles 380 and/or 381, which gives the irradiation times for the fluence shown in Table 2. The only exception was that the irradiation of the capsule at 935 °C to a fluence of 18.0×10^{24} n/m^2 ($E > 0.1$ MeV) was completed in cycle 382. No special shielding of the capsules was used, and the spectrum normally produced in HFIR in the PTP location was used for irradiation of the specimens with a nominal peak fast flux of 9.9×10^{18} n/m^2 s ($E > 0.1$ MeV), and a peak thermal flux of 2.2×10^{19} n/m^2 s ($E < 0.1$ MeV). However, the irradiation damage and dpa produced by the irradiation of molybdenum was primarily the result of the fast flux. The neutron fluence was determined from the number of effective full-power hours times the fast flux for the specific axial location of each respective capsule. The reported fluences apply to the gauge region of the specimen, but the variation in fluence along the length of the tensile specimen was estimated to be less than 0.1×10^{24} n/m^2 for the highest dose exposures. Transmutation of molybdenum after irradiation in HFIR was calculated to produce a very low concentration (<12 ppm) of elements (primarily Tc, Ru, Zr, Nb). The effect of these elements on the tensile properties was assumed to be negligible compared to the defects produced by neutron irradiation.

Determination of the irradiation temperatures is based on calculations of the specimen temperatures in the test capsule. The temperature of the tensile specimens is dependent on the size of the gas-gap from the

Table 2
Estimated irradiation temperature, neutron fluence, and calculated DPA values for LCAC molybdenum following irradiation in HFIR

Target irradiation temperature[a] (°C)	Tensile specimen irradiation temperature[b] (°C)	Neutron fluence ($E > 0.1$ MeV), $\times10^{24}$ n/m^2/(estimated molybdenum DPA)[c]		
LCAC molybdenum sheet				
300	265–270	10.5/(0.6)	N/A	N/A
600	585–605	16.2/(0.9)	27.0/(1.4)	N/A
1000	918–935	18.0/(1.0)	44.6/(2.4)	N/A
1200	1080–1100	22.9/(1.2)	44.7/(2.4)	61.3/(3.3)

N/A indicates that irradiations were not performed at these conditions.

[a] The target irradiation temperature was the aim calculated tensile specimen temperature that was designed for the irradiation test.

[b] The irradiation temperatures are the temperatures in the gauge region of the tensile specimen that were determined based on confirmatory data from SiC temperature monitors, with an estimated error of ±25 °C.

[c] The conversion from neutron fluence to molybdenum DPA for the HFIR spectrum was determined using SPECTER [17].

specimens to the filler pieces and from the filler pieces to the specimen holders. The irradiation temperatures were verified by taking post-irradiated electrical resistivity measurements from passive silicon carbide (SiC) temperature monitors after isochronous anneals [16], which were made in increments of 20 °C that were generally within the ±25 °C uncertainty of the temperature calculation. The SiC temperature monitors were $0.5 \times 1 \times 50$ mm rods that were positioned within the mid-diameter region of the holders that held the specimens in each capsule in a 1.2 mm diameter hole. Analysis of the SiC temperature monitors showed that the attained irradiation temperature was generally within 100 °C of the target irradiation temperature, as summarized in Table 2. The estimated variation of the irradiation temperature along the length of the tensile specimen was determined to be ±25 °C at the higher irradiation temperatures, and closer to ±15 °C at the lower irradiation temperature of 270 °C.

LCAC molybdenum was tensile tested in three conditions: (1) as-received to provide unirradiated control data, (2) thermally conditioned at the nominal irradiation temperature/time to evaluate the influence of thermal annealing, and (3) post-irradiated condition. Thermal conditioning of unirradiated material was performed by heat treatment in vacuum at the target irradiation temperatures for the period of irradiation time to evaluate the influence of the temperature exposure on the tensile properties: (1) 633 h at 300 °C, (2) 1232 h at 600 °C, (3) 1812 h at 1000 °C, and (4) 1726 h at 1200 °C. Tensile testing was performed at temperatures ranging from −150 to 1000 °C at an actuator displacement rate of 0.017 mm/s (strain rate = 0.05 min^{-1}) in accordance with ASTM E8 [18]. Specimen load and crosshead displacement were recorded and used to determine the 0.2% offset yield strength, ultimate tensile strength, uniform elongation, and total elongation. Room-temperature tests were conducted at atmospheric pressure, while elevated temperature tests and thermal conditioning were performed in a vacuum furnace ($<6 \times 10^{-5}$ MPa) that was equipped with refractory-metal heating elements and heat shields. Heating to the test temperature was typically achieved in 30–45 min, and each specimen was allowed to soak for at least 30 min at temperature prior to tensile testing. Tensile testing at sub-ambient temperatures was conducted in an environmental chamber that utilized cold nitrogen gas cooling to achieve temperatures down to −150 °C. Fractographic examinations were performed using scanning electron microscopy (SEM) to determine if the fracture was ductile or brittle in nature and to define the DBTT. Metallographic examination of the unirradiated specimens is also revealed using a Murakami etch (10 g potassium ferri-cyanide + 10 g potassium hydroxide + 100 ml water).

3. Results and discussion

3.1. Unirradiated tensile properties: as-received

Tensile results for unirradiated LCAC molybdenum are summarized in Table 3. The microstructure of LCAC molybdenum is shown in Fig. 2 to consist of elongated, sheet-like grains that are nominally 1–15 μm in diameter (average width = 3.9 μm) and aligned in the longitudinal direction with grain length ranging from 325 to 50 μm (average = 172 μm), while the grain size in the transverse direction ranged from 2 to 15 μm in diameter (average width = 5.0 μm) with length from 170 to 20 μm in diameter (average = 78.1 μm). Although the rolling used to form the LCAC molybdenum sheet produces an elongated grain structure, the yield strength and ultimate tensile strength values are closely similar for the longitudinal and transverse orientations. The recovery and formation of larger equiaxed grains during recrystallization (16.2 μm average diameter and 74.1 average length for longitudinal; 17.5 μm average diameter and 47.1 μm average length for transverse) results in a lower yield and ultimate tensile strength for LR and TR in comparison to LSR and TSR.

The load–displacement curves, which have not been corrected for the compliance of the load train, for LSR LCAC molybdenum tested at room-temperature show in Fig. 3 that a low work hardening rate (or strain hardening exponent, $n = 0.08$ to 0.008) is observed for LCAC molybdenum, as reported in the literature [1–11,19,20]. The wide spacing of sheet-like grains and smaller grain width for the TSR orientation results in more grain boundary area in the tensile direction for fracture initiation, which likely results in slightly lower total elongation values compared to LSR LCAC. The fracture surface of LSR is relatively flat, and consists of a laminate type fracture with necking of sheet-like grains (see Fig. 4(a)). The fracture of LSR LCAC molybdenum likely initiates at grain boundaries between the sheet-like grains, and the sheet-like grains are then pulled to necking failure to result in the laminate fracture appearance. A ductile fracture and measurable amounts of total elongation were observed for LSR and TSR LCAC molybdenum at −100 °C, while brittle fracture and little tensile ductility were observed at a temperature of −150 °C, which indicates that the DBTT for LSR and TSR LCAC is −100 °C.

The load–displacement curves for tensile testing of LR LCAC molybdenum at room-temperature are shown in Fig. 3 to exhibit both an upper and lower yield point (Lüders' plateau) followed by a low work hardening rate (strain hardening exponent, $n = 0.16$ to 0.31) that is higher than LSR. The trapping of dislocations by the atmospheres of impurity solute atoms (i.e. carbon) is reported to result in the formation of an upper and

Table 3
Summary of unirradiated tensile data for LCAC molybdenum sheet

Test temperature (°C)	Tensile strength (MPa)		Tensile ductility (%)	
	Ultimate tensile stress	0.2% yield stress	Total elongation	Uniform elongation
Longitudinal stress relieved				
−150	1554.8	1554.8	<1	<1
−100	1226.6	1226.6	14	<1
−50	992.2	997.7	18	<1
0	801.2	832.2	18	10
22	797.8	743.3	18	10
22	788.1	762.6	16.2	7.4
22	792.9	756.4	18.9	6.3
23	800.5	750.9	16	7
300	588.8	523.3	5.3	2.6
300	577.1	508.9	6.8	3.6
600	529.5	482.7	4.2	1.7
600	515.7	519.9	3.0	0.9
1093	136.5	110.3	23	Not reported
Longitudinal recrystallized				
22[a]	526.1	538.5	27.5	11.9
22[a]	541.9	539.9	30.6	12.1
300	294.4	104.1	33.0	30.1
300	289.6	109.6	35.3	30.9
600	230.3	92.4	30.4	27.1
600	231.7	118.6	31.4	27.5
1093	137.9	78.6	29	17
Transverse stress relieved				
−150	1592.7	1592.7	<1	<1
−100	1307.3	1319.0	9	<1
−50	1067.3	1073.6	15	<1
RT[a]	792.2	828.8	14	6
22	839.8	789.5	10	6
22	841.9	809.5	15.4	5.2
871	239.9	236.5	6	1
Transverse recrystallized				
22[a]	549.5	568.1	26.2	10.3
22[a]	546.1	559.9	22.3	9.3

[a] The upper/lower yield point observed for this result in a high value for the yield stress. Ultimate tensile stress is the highest stress following the upper/lower yield point, which can be lower than or comparable to the yield stress in some cases.

lower yield point in molybdenum [19,20]. The higher work hardening rate for LR and TR LCAC molybdenum may result in more resistance to plastic instability, and produce the slightly higher total elongation values. The fracture surface of LR is shown in Fig. 4(b) to exhibit a ductile laminate fracture surface with necking of the sheet-like grains, which is likely produced by fracture initiation at grain boundaries to leave ligaments of sheet-like grains that are pulled to necking failure. The laminates observed on the fracture surface of LR LCAC are more curved and thicker than observed for LSR, and a few regions of transgranular cleavage are observed, which is attributed to the larger grain size of LR. LSR had a finer grain size, and no evidence of transgranular cleavage was observed at the fracture surface in Fig. 4(a).

The large total elongation and ductile failure observed for LR and TR LCAC at room-temperature indicates that the DBTT is below room-temperature. A decrease in the yield and ultimate tensile strength is observed for the tensile testing of LSR and LR molybdenum at temperatures above room-temperature (see Table 3) [1–11,19,20]. The load–displacement curves for LR LCAC molybdenum tested at 300 and 600 °C show in Fig. 3 that the Lüders' plateau was absent and a low strain hardening exponent ($n = 0.26$ to 0.31) was observed.

3.2. Unirradiated tensile properties: thermal conditioning

The decrease in hardness versus annealing temperature shows in Fig. 5 that the onset of recrystallization

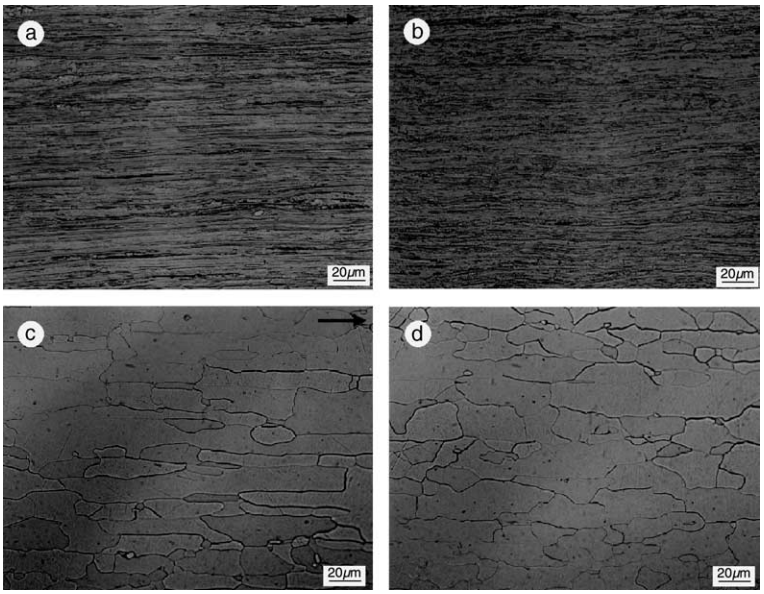

Fig. 2. Polished and etched optical micrographs of the microstructure of LCAC molybdenum sheet: (a) longitudinal orientation in the stress-relieved condition (LSR), (b) transverse orientation in the stress-relived condition (TSR), (c) longitudinal orientation in recrystallized condition (LR), and (d) transverse orientation in the recrystallized condition (TR). A Murakami etch was used. The arrow identifies the longitudinal direction.

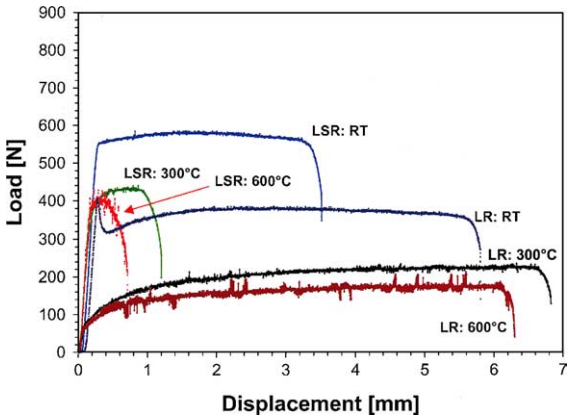

Fig. 3. Load–displacement curves obtained for the tensile testing of unirradiated LSR and LR LCAC molybdenum sheet at room-temperature, 300 and 600 °C. The work hardening rates determine from plots of true stress–strain are: (1) LSR/RT, $n = 0.076$; (2) LSR/300 °C, $n = 0.056$; (3) LSR/600 °C, $n = 0.0076$; (4) LR/RT, $n = 0.16$; (5) LR/300 °C, $n = 0.31$; (6) LR/600 °C, $n = 0.26$.

was observed for LCAC molybdenum at approximately 1000 °C. The irradiation temperature of 600 °C is well below the respective recrystallization temperature for LCAC, and no change in tensile properties, DBTT, or fracture mode was observed after vacuum annealing at 600 °C for times that are comparable to the irradiation exposures (Fig. 6). Recrystallization of LCAC molybdenum is observed following vacuum annealing at 1000 °C, and the tensile properties of LSR are shown in Fig. 6 to be comparable to LR LCAC molybdenum. This indicates that any change in the mechanical properties of LCAC molybdenum following irradiation at temperatures 600 °C are the result of the radiation effects alone. Irradiation of LCAC molybdenum at temperatures $\geqslant$1000 °C will be influenced by recrystallization.

3.3. Post-irradiation tensile properties for irradiation at 270 and 605 °C

Tensile data obtained for stress-relieved and recrystallized LCAC molybdenum sheet following irradiation are summarized in Tables 4 and 5, respectively. The tensile properties for LSR and LR LCAC molybdenum in the unirradiated, 270 °C irradiated and 605 °C irradiated are compared in Fig. 7. The yield strength and ultimate tensile strength values are significantly increased by irradiation of LCAC molybdenum at 270 °C (increases ranging from 88% to 160%), while a smaller increase in strength was observed for the 605 °C irradiation (39–124%). The higher yield and ultimate tensile strength for LSR material in comparison to the LR condition was maintained before and after irradiation at 270 and 605 °C, but the relative percent increase in strength for the LSR and LR was comparable. A significant decrease in elongation to values near zero is shown in Figs. 7(b) and 8(a) for tensile testing of 270 °C irradiated LSR and LR at room-temperature and 300 °C,

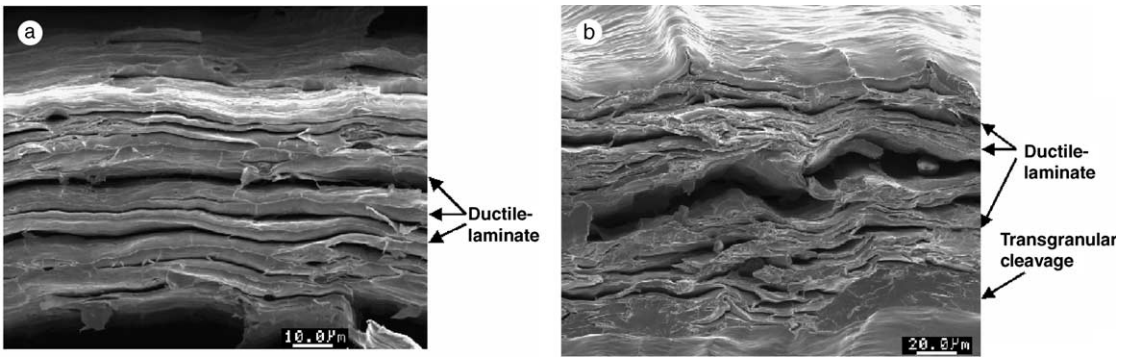

Fig. 4. SEM fractography of unirradiated LCAC molybdenum specimens that were tensile tested at room-temperature: (a) LSR specimen and (b) LR specimen. Both show a ductile-laminate failure mode of the pancake shaped grains that are inherent to the microstructure.

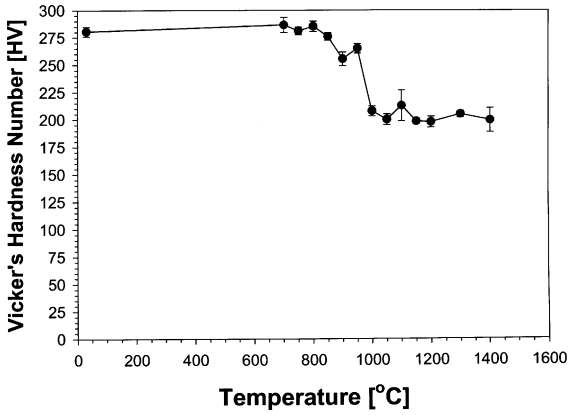

Fig. 5. Plot of the effect of one hour annealing on the microhardness of LCAC molybdenum sheet. The data points are an average of ten readings, with the error bars representing 1 standard deviation.

while limited ductility was observed for LR LCAC that was tested at 600 °C.

The 605 °C irradiated LSR and LR LCAC molybdenum showed a decrease in elongation to values near zero for room-temperature tensile testing, while little change in elongation was observed for tensile testing of LSR at 300 and 600 °C. Brittle fracture by transgranular cleavage was observed for 270 °C irradiated LSR and LR LCAC after tensile testing at room-temperature and 300 °C (see Fig. 9(a)). Similarly, brittle fracture with transgranular cleavage is shown in Fig. 10(a) for the room-temperature tensile testing of LCAC after irradiation at 605 °C. These results show that the grain boundaries in the LCAC molybdenum were not embrittled by irradiation, as an intergranular fracture path was not observed. The fracture initiation sites are identified as small linear defects that are likely a microcrack or grain boundary. Embrittlement of molybdenum irradiated at temperatures <700 °C may result in

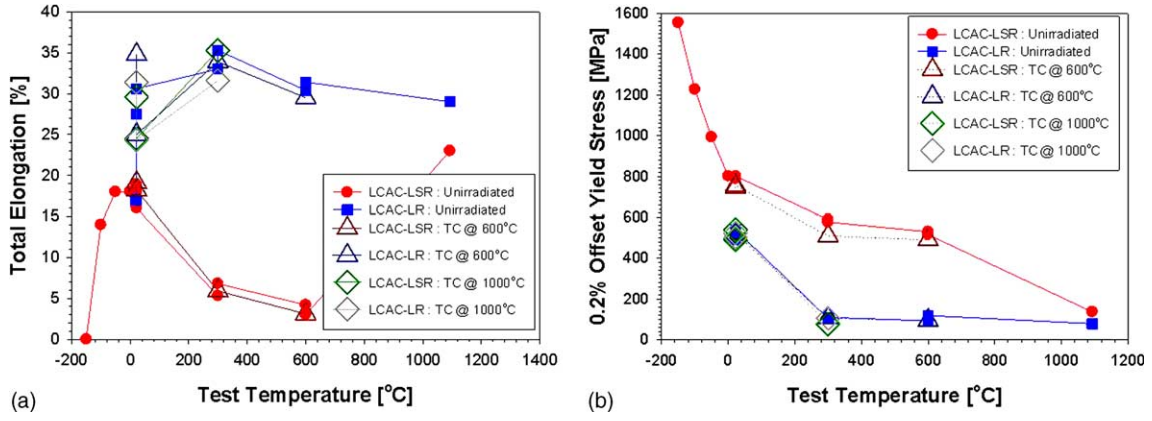

Fig. 6. Plot of non-irradiated and non-irradiated + thermally conditioned tensile properties versus test temperature for LCAC molybdenum sheet in the LSR and LR condition: (a) yield strength and (b) total elongation. Thermal conditioning was performed by vacuum annealing at 600 and 1000 °C for times comparable to the irradiation exposure.

Table 4
Summary of irradiated tensile data for stress-relived LCAC molybdenum sheet

Irradiation temperature (°C)	Neutron fluence (n/m^2), $E > 0.1$ MeV	Test temperature (°C)	Tensile strength (MPa)		Tensile ductility (%)	
			Ultimate tensile stress	0.2% yield stress	Total elongation	Uniform elongation
Longitudinal stress relieved						
270	10.5×10^{24}	22	1501.7	1486.6	0.12	0.07
270	10.5×10^{24}	22	1516.9	1510.0	0.37	0.13
270	10.5×10^{24}	300	1098.4	1098.4	0.00	0.00
605	16.2×10^{24}	22	822.6	846.7	0.75	0.31
605	16.2×10^{24}	22	910.8	920.5	0.27	0.02
605	27.0×10^{24}	22	1042.5	1050.8	0.24	0.19
605	16.2×10^{24}	300	632.3	596.4	2.52	1.13
605	27.0×10^{24}	300	919.8	841.9	5.35	3.95
605	16.2×10^{24}	600	766.7	698.5	3.16	2.06
605	27.0×10^{24}	600	861.9	770.2	4.37	3.11
935	18.0×10^{24}	22	517.1	540.6	4.4	3.1
935	18.0×10^{24}	22	602.6	645.4	5.3	1.3
935	44.6×10^{24}	22	507.5	537.1	12.6	7.1
935	18.0×10^{24}	300	399.9	291.7	11.0	9.3
935	44.6×10^{24}	300	211.0	202.0	5.9	2.9
1100	61.3×10^{24}	22	457.1	506.1	23.0	9.8
1100	61.3×10^{24}	22	497.1	527.5	20.1	9.4
1100	61.3×10^{24}	300	252.4	173.8	22.3	20.0
Transverse stress relieved						
1100	61.3×10^{24}	22	531.6	556.4	12.5	8.3
1100	61.3×10^{24}	22	523.3	515.7	17.6	9.1

the formation of small microcracks at grain boundaries or within the grains during tensile loading that serve as fracture initiation sites. A small amount of ductility is observed in Fig. 8(a) for 270 °C irradiated LR LCAC molybdenum following tensile testing at 600 °C, and the fracture surface shown in Fig. 9(b) exhibits necking and dimpled rupture. This indicates that the DBTT of 270 °C irradiated LCAC molybdenum is less than or equal to 600 °C and higher than 300 °C, but is conservatively identified to be 600 °C. Measurable elongation was observed for the 605 °C irradiated tensile specimen after testing at 300 °C (Fig. 8(a)), and a ductile, laminate-type fracture is shown in Fig. 10(b), which indicates that the DBTT is $\leqslant$300 °C and >room-temperature, but is conservatively identified to be 300 °C.

The large increase in the tensile strength and decrease in tensile ductility for room-temperature tensile testing of 605 °C irradiated LSR LCAC molybdenum is observed after a fluence of 16.2×10^{24} n/m^2 ($E > 0.1$ MeV), with little change in tensile properties between the 16.2×10^{24} and 27.0×10^{24} n/m^2 fluence exposure, which indicates that the tensile properties for LSR LCAC have been saturated at a neutron fluence $\leqslant16.2\times10^{24}$ n/m^2. A small increase in tensile strength and decrease in ductility was observed for the room-temperature tensile test of LR LCAC after irradiation to a fluence of 16.2×10^{24} n/m^2, but the fracture was ductile. Additional increases in tensile strength and decrease in tensile elongation with brittle fracture by transgranular cleavage was observed for room-temperature tensile tests of 605 °C irradiated LR LCAC after a neutron fluence of 27.0×10^{24} n/m^2. This indicates that saturation of the change in the tensile properties of 605 °C irradiated LR LCAC occurs between a neutron fluence of 16.2×10^{24} and 27.0×10^{24} n/m^2. The larger grain size and initial recovered microstructure that is associated with LR LCAC molybdenum in comparison to LSR LCAC may result in the delay of saturation of the tensile properties to a higher fluence of 27.0×10^{24} n/m^2 for the 605 °C irradiation temperature. However, transgranular cleavage with similar initiation sites was observed at the fracture surface for both LSR and LR specimens that were tested at room-temperature after irradiation at temperatures $\leqslant$605 °C, which indicates that the general mechanism of irradiation embrittlement is the same.

Since the solid-state diffusion rate and mobility of the vacancies and interstitials that are formed by irradiation of molybdenum at temperatures <800 °C is lower than observed at higher temperature, annihilation of point defects at sinks (grain boundaries, precipitate bound-

Table 5
Summary of irradiated tensile data for recrystallized LCAC molybdenum sheet

Irradiation temperature (°C)	Neutron fluence (n/m^2), $E > 0.1$ MeV	Test temperature (°C)	Tensile strength (MPa)		Tensile ductility (%)	
			Ultimate tensile stress	0.2% yield stress	Total elongation	Uniform elongation
Longitudinal recrystallized						
270	10.5×10^{24}	22	984.6	984.6	0.05	0.01
270	10.5×10^{24}	22	1039.1	1039.1	0.02	0.01
270	10.5×10^{24}	600	629.5	591.6	1.02	0.14
605	16.2×10^{24}	22	686.7	669.5	6.3	3.9
605	16.2×10^{24}	22	676.4	658.5	6.6	4.7
605	27.0×10^{24}	22	811.5	808.8	1.19	1.12
605	27.0×10^{24}	22	852.9	852.9	0.21	0.06
935	18.0×10^{24}	22	622.6	651.6	12.6	7.2
935	18.0×10^{24}	22	566.1	630.9	15.4	8.3
935	44.6×10^{24}	22	529.5	548.2	18.0	9.1
935	44.6×10^{24}	22	525.4	553.0	15.0	8.3
1100	22.9×10^{24}	22	446.8	424.0	19.5	10.7
1100	22.9×10^{24}	22	450.2	417.1	23.7	11.6
1100	44.7×10^{24}	22	427.5	408.9	24.0	9.2
1100	44.7×10^{24}	22	435.8	370.3	27.9	13.7
1100	61.3×10^{24}	22	480.6	464.0	27.9	7.5
1100	61.3×10^{24}	22	455.1	488.2	22.4	10.2
Transverse recrystallized						
1100	61.3×10^{24}	22	521.3	538.5	22.0	10.7

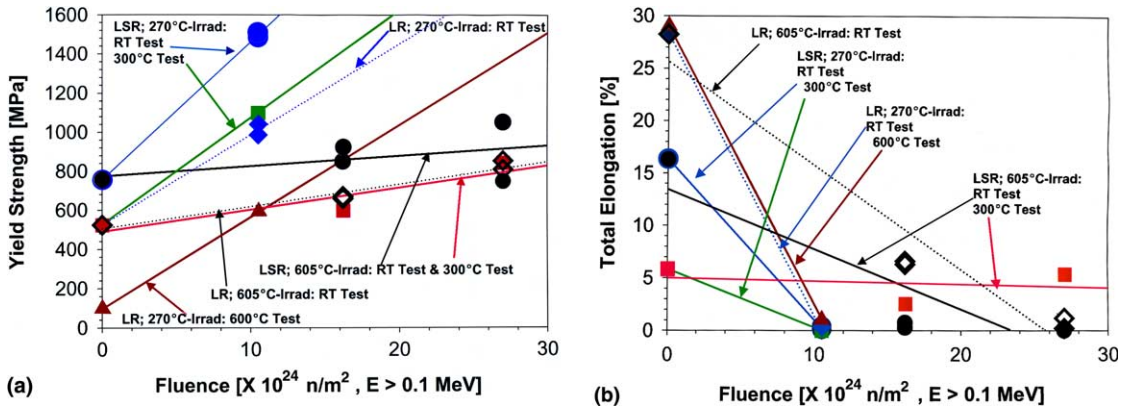

Fig. 7. Comparison of irradiated and unirradiated tensile data for the LCAC molybdenum sheet in the LSR and LR condition after: (1) irradiation at 270 °C for tensile testing of LSR performed at room-temperature and 300 °C and tensile testing of LR at room-temperature and 600 °C, and (2) irradiation at 605 °C for tensile testing of LSR at room-temperature and 300 °C and tensile testing of LR at room-temperature. Unirradiated data are shown by average values at zero fluence for as-received material. The tensile data shown are: (a) 0.2% yield strength and (b) total elongation. The lines are a linear regression fit to the data.

aries, dislocations, etc.) occurs at a much slower rate than the production rate. This results in the formation of finely spaced clusters of point defects or fine dislocation loops during the irradiation of molybdenum at temperatures less than 800 °C (black spot damage) [1–8]. The large increase in the tensile strength with a significant loss of ductility is observed for LCAC molybdenum after irradiation at temperatures $\leqslant$605 °C that is similar to that reported in literature [1–8,21–29]. Irradiation embrittlement is shown by the increase in the DBTT of

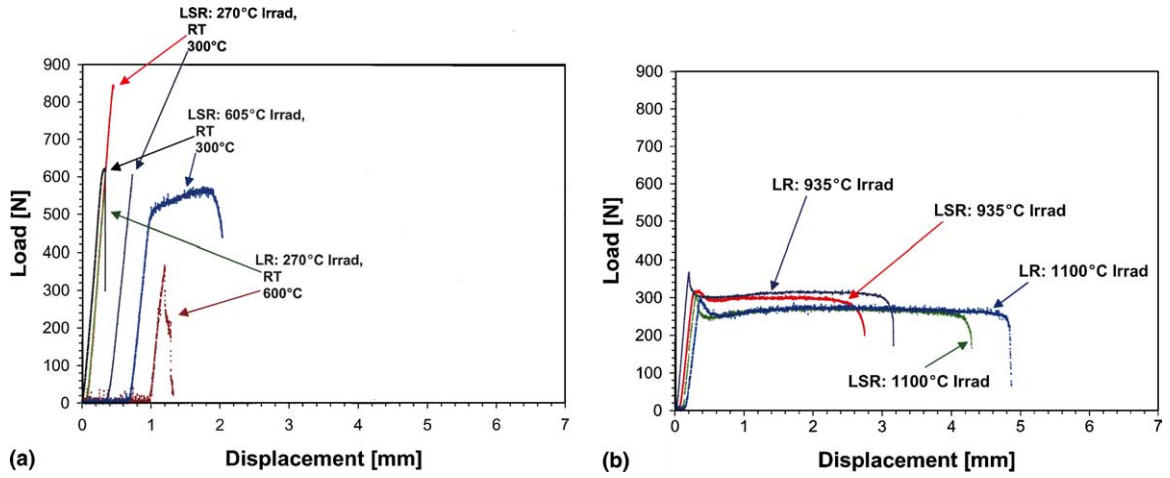

Fig. 8. Load–displacement curves obtained for the tensile testing of LSR and LR LCAC molybdenum following irradiation at: (a) 270 °C to a fluence of 10.5×10^{24} n/m^2 and 605 °C to a fluence of 27.0×10^{24} n/m^2, tensile testing was performed from room-temperature to 600 °C, and (b) 935 °C to a 44.6×10^{24} n/m^2 and 1100 °C to a fluence of 61.3×10^{24} n/m^2, tensile testing was performed at room-temperature. Load–displacement curves for unirradiated data are shown in Fig. 3 using the same scale for comparison. The work hardening rates determine from plots of true stress–strain are: (1) 270 °C-irradiation: LR/600 °C, $n = -4.4$; (2) 605 °C-irradiation, LSR/300 °C, $n = 0.25$; (3) 935 °C-irradiation: LSR/RT, $n = 0.071$ and LR/RT, $n = 0.093$; (4) 1100 °C-irradiation, LSR/RT, $n = 0.10$ and LR/RT, $n = 0.11$.

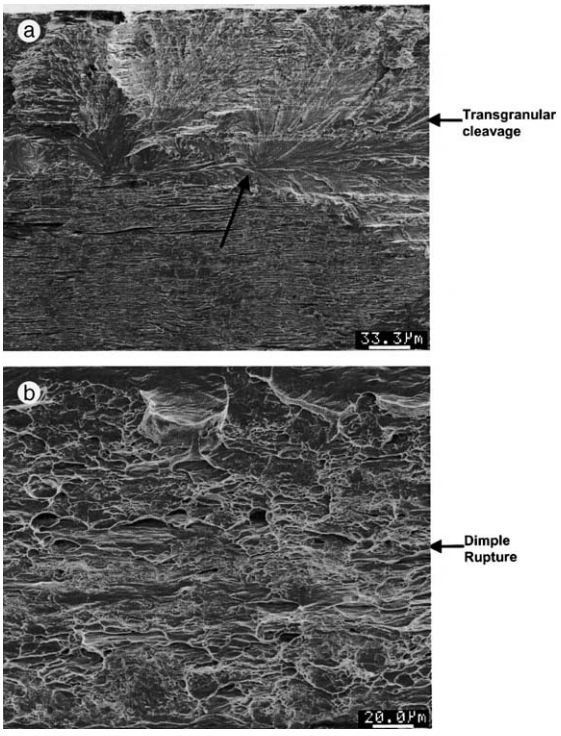

Fig. 9. SEM fractography of a LCAC molybdenum specimen that was tensile tested after irradiation at 270 °C to a nominal fluence of 10.5×10^{24} n/m^2 ($E > 0.1$ MeV): (a) LSR specimen tested at 300 °C, lower magnification image of the fracture initiation site (indicated by the arrow), and (b) LR specimen tested at 600 °C showing dimple rupture.

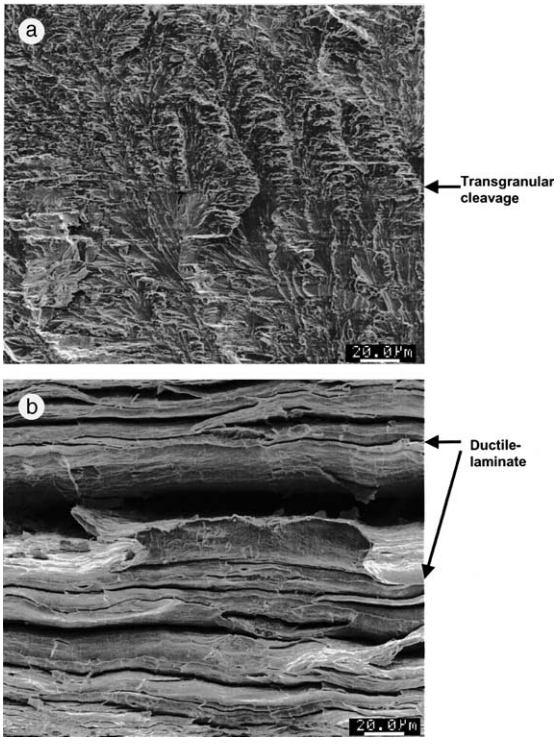

Fig. 10. SEM fractography of a LCAC molybdenum specimen that was tensile tested after irradiation at 605 °C to a nominal fluence of 27.0×10^{24} n/m^2 ($E > 0.1$ MeV): (a) LSR specimen tested at room-temperature, higher magnification image of the fracture initiation site, and (b) LSR specimen tested at 300 °C.

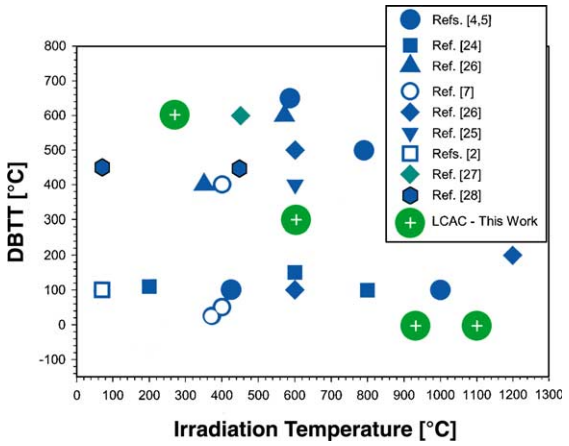

Fig. 11. Summary of literature data for molybdenum showing a plot of DBTT versus irradiation temperature. The DBTT for LCAC in this work is shown by the large circles with plus in middle for irradiations at 270, 605, 935, and 1100 °C. The DBTT for LCAC irradiated at 935 and 1100 °C is below room-temperature. Note, the DBTT values determined for irradiation at 270 and 605 °C are conservatively estimated to be 600 and 300 °C, respectively, but the true values could be 300 °C < DBTT $\leqslant$ 600 °C for the 270 °C irradiation and room-temperature < DBTT $\leqslant$ 300 °C for the 605 °C irradiation.

LCAC from below room-temperature prior to irradiation to 600 and 300 °C after irradiation at 270 and 605 °C, respectively. Literature data reported for irradiation of molybdenum at 300–400 °C to a lower neutron fluence than used in this work gives a DBTT ranging from 70 to 400 °C (see Fig. 11). Irradiation to the higher neutron fluences used for the 270 °C irradiation in this work may be needed to achieve a saturation density of the defects that result in the DBTT (600 °C) observed here. The DBTT of 605 °C irradiated LCAC molybdenum determined from this work (conservatively as 300 °C) is shown in Fig. 11 to be at the lower end of the range in DBTT values (100–650 °C) reported in literature. This result indicates that the LCAC molybdenum evaluated in this work exhibits some limited resistance to radiation embrittlement. Intergranular fractures are generally associated with a high DBTT for molybdenum. Use of arc-cast processing, a fine grain size in the wrought product, low oxygen content, and high carbon to oxygen ratio for LCAC molybdenum appears to prevent the weakening of grain boundaries to result in a transgranular fracture mode.

3.4. Post-irradiation tensile properties for irradiation at 935 and 1100 °C

The tensile properties for 935 and 1100 °C irradiated LCAC molybdenum are compared with unirradiated material for tensile testing performed at room-temperature in Fig. 12. Since thermal exposure of LCAC molybdenum at 1000 °C results in recrystallization, the thermally conditioned data were used as the unirradiated baseline data. Fig. 12 shows that little net change [small increase (1% to 28%) or decrease (−2% to −57% decrease) in values] in the yield strength and total elongation was generally observed for LCAC molybdenum after irradiation at 935 and 1100 °C. The only exception to these ranges are the decrease in total elongation and uniform elongation values for tensile testing of 935 °C irradiated LSR LCAC molybdenum, where a larger initial decrease in elongation was observed after a neutron fluence of 18.0×10^{24} n/m^2. However, measurable elongation and a ductile failure are observed, and little change in elongation is observed between the irradiation fluences of 18.0 and 44.6×10^{24} n/m^2 for the 935 °C irradiation, which indicates that little hardening may occur at longer fluence exposures at a 935 °C irradiation temperature. Little change in tensile properties was observed for the LSR, TSR, LR, and TR metallurgical conditions of LCAC molybdenum after irradiation at 1100 °C, which indicates that radiation effects are similar in the longitudinal and transverse orientation for LCAC at a 1100 °C irradiation temperature.

The load–displacement curves for 935 and 1100 °C irradiated LSR and LR LCAC molybdenum tensile tested at room-temperature show in Fig. 8(b) that the tensile properties are generally comparable to unirradiated recrystallized LCAC (Fig. 3). The upper/lower yield point occurs over a slightly longer displacement for the room-temperature tensile test of the 935 and 1100 °C irradiated LSR and LR, but the low strain hardening exponent ($n = 0.07$ to 0.11) observed for the irradiated material is within a factor of ~2 of the unirradiated LR at room-temperature ($n = 0.16$). These slight differences in the load–displacement curves likely result from the irradiation defects inhibiting dislocation motion. The fracture surfaces for the room-temperature tensile testing of the 935 and 1100 °C irradiated LSR and LR LCAC show in Fig. 13 a high degree of necking that is comparable to the unirradiated recrystallized LCAC (Fig. 4(b)). The point defects that are produced by irradiation at 935 and 1100 °C have a high enough mobility for rapid solid-state diffusion to sinks for annihilation to occur, and results in the formation of voids that appear to have little influence on the tensile properties [1–10]. A mixed-mode fracture consisting of ductile-laminate type failure of sheet-like grains and transgranular cleavage was observed, with a lower fraction of transgranular cleavage type features observed on the fracture surface of the irradiated LR compared to LSR. Nonetheless, these failures are assumed to be ductile. Recrystallization of LSR occurs during irradiation at 935 and 1100 °C while the LR was in a recrystallized condition prior to irradiation. The

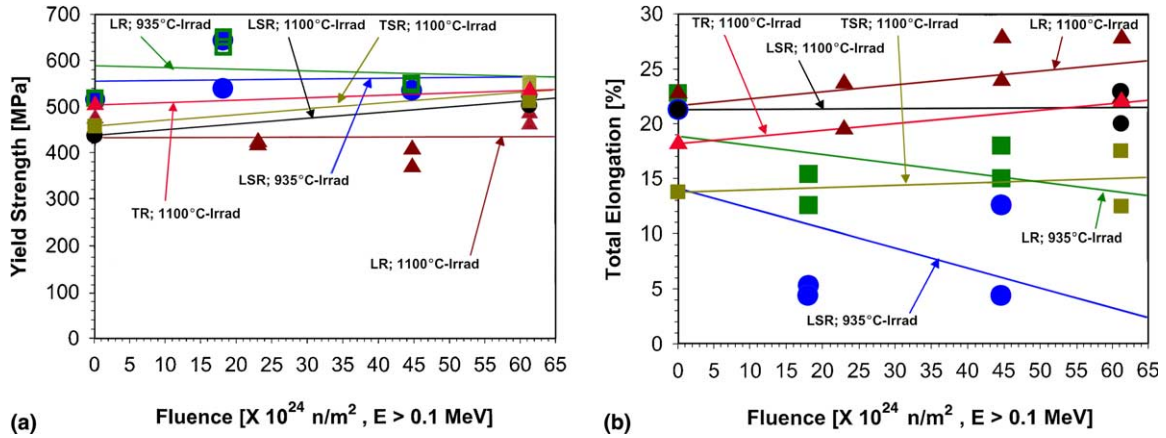

Fig. 12. Comparison of room-temperature tensile data for irradiated and unirradiated LCAC molybdenum sheet after: (1) irradiation at 935 °C for LSR and LR, and (2) irradiation at 1100 °C for LR, LSR, TSR, and TR. Unirradiated data are shown by average values at zero fluence for as-received and 1000 and 1200 °C thermally conditioned material. The tensile data shown are: (a) 0.2% yield strength and (b) total elongation. The lines are a linear regression fit to the data.

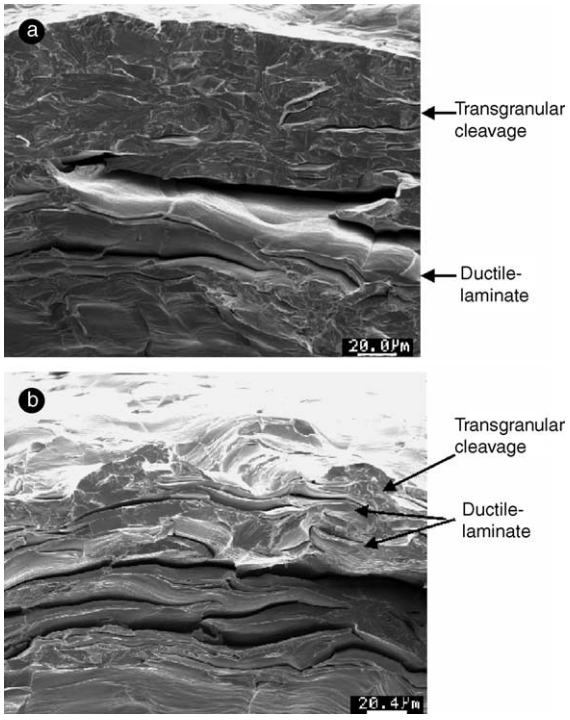

Fig. 13. SEM fractography of a LSR LCAC molybdenum specimen that was tensile tested at room-temperature after irradiation under the following conditions: (a) irradiation at 935 °C to a nominal fluence of 44.7×10^{24} n/m^2, and (b) irradiation at 1100 °C to a nominal fluence of 61.3×10^{24} n/m^2.

improved microstructural stability of LR may explain the higher amount of elongation and greater fraction of ductile failure compared to the LSR condition. The measurable amount of total elongation and ductile failure mode that is observed following room-temperature tensile testing of the 935 and 1100 °C irradiated LCAC indicates that the DBTT is below room-temperature, which is below the values reported in literature (Fig. 11).

4. Summary

The unirradiated yield and ultimate tensile strength properties for LCAC molybdenum are generally lower at temperatures above room-temperature. The start of the recrystallization of LCAC molybdenum for a 1-h heat treatment is 1000 °C, and the tensile properties of LCAC that is irradiated at 935 and 1100 °C were influenced by recrystallization and recovery.

Irradiation of LCAC molybdenum at 270 and 605 °C results in a large increase in the room-temperature yield strength (from 763–743 to 1517–821 MPa) and decrease in total elongation to values near zero. The largest increases in room-temperature yield strength were observed for the 270 °C irradiation with less strengthening observed for the 605 °C irradiation. Similar tensile properties have been observed in literature for molybdenum irradiated at temperatures $\leqslant$800 °C. The DBTT of 270 °C irradiated LCAC molybdenum was determined by tensile tests to conservatively be 600 °C, while the DBTT of 605 °C irradiated LCAC was conservatively estimated to be 300 °C. Intergranular fractures are generally associated with a high DBTT for molybdenum irradiated at temperatures <800 °C. The brittle fractures for LCAC molybdenum occurred by transgranular

cleavage that was initiated from small linear defects, which indicates that the use of arc-cast processing, fine grain size, a low oxygen content, and high carbon to oxygen ratio result in strong grain boundaries that are not the preferred fracture path.

Irradiation of LCAC molybdenum at 935 and 1100 °C results in a slight change in tensile properties with no change in the DBTT and fracture surface compared to unirradiated recrystallized LCAC molybdenum. The DBTT values determined for LCAC molybdenum after irradiated at temperatures >900 °C are less than reported in literature for irradiation of molybdenum at 800–1200 °C. However, saturation of the tensile properties with neutron fluence was not observed, and irradiation of LCAC molybdenum at temperatures >800 °C to higher neutron fluences could result in further increases in the DBTT. Higher total elongation and more ductile fractures were observed for recrystallized (LR and TR) LCAC molybdenum following irradiation at 935 and 1100 °C compared to stress-relived (LSR and TSR) material, which are explained by the large changes in the microstructure and recrystallization that occur for LSR and TSR material. Use of recrystallized LCAC molybdenum would be preferred for applications that involve prolonged irradiation exposures at temperatures >900 °C.

Acknowledgements

This work was supported under USDOE Contract No. DE-AC11-98PN38206. The assistance of R.F. Luther in providing the LCAC molybdenum specimens used in this work is appreciated. Thanks to the following ORNL personnel for completing this work (J.P. Strizak, T.S. Byun, A.L. Qualls, A.W. Williams, and J.L. Bailey).

References

[1] V.K. Sikka, J. Moteff, Nucl. Tech. 22 (1974) 52.
[2] K. Furuya, J. Moteff, Metall. Trans. A 12 (1981) 1303.
[3] J.A. Sprague et al., J. Nucl. Mater. 85&86 (1979) 739.
[4] B.L. Cox, F.W. Wiffen, J. Nucl. Mater. 85&86 (1979) 901.
[5] F.W. Wiffen, in: R.J. Arsenault (Ed.), Proceedings of the 1973 International Conference on Defects and Defect Clusters in B.C.C. Metals and Their Alloys, Nuclear Metallurgy, vol. 18, 1973, p. 176.
[6] R.E. Gold, D.L. Harrod, J. Nucl. Mater. 85&86 (1979) 805.
[7] A. Hasegawa et al., J. Nucl. Mater. 233–237 (1996) 565.
[8] B.N. Singh et al., J. Nucl. Mater. 212–215 (1994) 1292.
[9] Standard specification for molybdenum and molybdenum alloy plate, sheet, strip, and foil, ASTM B386-95, American Society for Testing and Materials, Philadelphia, PA, 1997.
[10] M. Semchyshen, R.Q. Barr, J. Less-Common Metals 11 (1966) 1.
[11] B. Mastel, J.L. Brimhall, Acta Metall. 13 (1965) 1109.
[12] A. Kumar, B.L. Eyre, Proc. R. Soc. Lond. A 370 (1980) 431.
[13] H. Kurishita, H. Yoshinaga, Mater. Forum 13 (1989) 161.
[14] B.V. Cockeram, Metall. Trans. A 33 (2002) 3685.
[15] J.A. Shields, P. Lipetzky, A.J. Mueller, in: G. Kneringer, P. Rodhammer, H. Wildner (Eds.), Proceedings of the 15th International Plansee Seminar, vol. 4, Plansee Holding AG, Reutte, Austria, 2001, p. 187.
[16] L.L. Snead, S.J. Zinkle, Nucl. Instrum. and Meth. B 191 (2002) 497.
[17] L.R. Greenwood, R.K. Smither, Specter: neutron damage calculations for materials irradiations, ANL/FPP/TM-197, Argonne National Laboratory, January 1985.
[18] Standard test methods for tension testing of metallic materials, ASTM E8-01, American Society for Testing and Materials, Philadelphia, PA, 2001.
[19] A. Lawley, J. Van den Sype, R. Maddin, J. Inst. Metals 91 (1962–1963) 23.
[20] G.W. Brock, Trans. Metall. Soc. AIME 221 (1961) 1055.
[21] I.V. Gorynin et al., J. Nucl. Mater. 191–194 (1992) 421.
[22] B.N. Singh et al., J. Nucl. Mater. 258–263 (1998) 865.
[23] A. Hasegawa et al., J. Nucl. Mater. 225 (1995) 259.
[24] K. Watanabe et al., J. Nucl. Mater. 258–263 (1998) 848.
[25] K. Abe et al., J. Nucl. Mater. 99 (1981) 25.
[26] V. Chakin, V. Kazakov, J. Nucl. Mater. 233–237 (1996) 570.
[27] K. Abe et al., J. Nucl. Mater. 122&123 (1984) 671.
[28] N. Igata, A. Kohyama, K. Itadani, J. Nucl. Mater. 85&86 (1979) 895.
[29] M. Scibetta, R. Chaouadi, J.L. Puzzolante, J. Nucl. Mater. 283–287 (2000) 455.